UDC 539.4

Finite Element Method for Evaluating Rising and Slip of Column–Base Plate for Usual Connections

M. Hamizi,[a,1] H. Ait-Aider,[a,2] and A. Alliche[b,3]

[a] Université Mouloud Mammeri de Tizi Ouzou, Algérie

[b] Université Pierre et Marie Curie Paris VI, Paris, France

[1] chamizi@yahoo.fr

[2] h_aitaider@yahoo.fr

[3] abdenour.alliche@upmc.fr

УДК 539.4

Конечноэлементный метод оценки деформирования и проскальзывания креплений стальной колонны к основанию

М. Хамизи[а], Х. Эйт-Эйдер[а], А. Аллиш[б]

[а] Университет им. Мулуда Маммери, Тизи-Узу, Алжир

[б] Университет им. Пьера и Мари Кюри, Париж, Франция

Предложена конечноэлементная методика расчета деформирования и относительного проскальзывания креплений стальной колонны к железобетонному основанию. Рассмотрены два случая крепления: пластина приваривается к торцу колонны и крепится двумя или четырьмя анкерными болтами к железобетонному основанию. В конечноэлементной модели с использованием модифицированного метода Лагранжа учитывается растрескивание бетонного основания и эффекты трения. Деформирование бетонного основания описывается с помощью упругопластической модели сжатия материала. По результатам расчетов построены диаграммы перемещений элементов крепления.

Ключевые слова: соединения, основание, метод конечных элементов, проскальзывание, бетонное основание, упругопластическая модель.

Introduction. In column-beam connections, the base plate is necessary to transmit the effort acting in the column to the reinforced concrete foundation. The dimensions of the base plate ($b \times d$) are given by considering the pressure transmitted to the subjacent concrete, which must resist without rupture. The thickness of the base plate t_p is given by considering the pressure transmitted by the concrete. The number of anchor bolts, the space between bolts just as the welding connecting the column to the base plate are other factors which can influence the choice of dimensions of the base plate. The dimensioning of the base plate is a relatively simple work if one has tables and scheme solvers like those proposed by Stockwell [1], Sandhu [2], Bird [3], C.M. 66 [4], Eurocode [5]. The recent studies, both experimental and numerical, have shown that other parameters like rising and slip could affect the base plate behavior. The rising and slip are generated by the contact between the base and the reinforced concrete foundation.

In the last decades, a significant work dealing with the problem of rising and slip between base plate and reinforced concrete foundation has been carried out by many researches. Several approaches were used: experimental, analytical and numerical ones. The laboratory tests have confirmed that separation of the connection always occurred at the level surface of contact between the base plate and reinforced concrete foundation which is treated as fully rigid connection [6–8]. Other experimental studies under concentrated loads and offset loads describing and evaluating the response of the column base connections were carried out [9–12]. The analytical approach, on the other hand, based on a variable distribution of the reaction of the reinforced concrete foundation on the base plate under a low concentrated load applied in the top of the column gave a significant surface of contact [13, 14]. Another approach, by the finite element method, to evaluate the rising and the slip of the base plate compared to the reinforced concrete foundation has been implemented recently [15, 16]. Several models were used. The unidimensional model based on the theory of Bernoulli with spring simulation of the anchor bolt yielded somewhat mitigated results [17]. On the other hand, models with two (2D) and three dimensions (3D) have been used, which had the following advantages:

(i) visualization of normal and tangential displacement;

(ii) precise numerical results;

(iii) minimal costs of data processing.

The results obtained by the above models have provided adequate assessment of rising and slip between the base plate and the reinforced concrete foundation [18–25].

1. **Development of the Finite Element Model**. Taking into account studies enumerated above and various recommendations, a three-dimensional finite element model based on the nonlinear analysis of the structure to simulate the behavior of column–base plate connection is proposed in this study. The model takes into account nonlinearity of materials and nonlinearity of contact between the foundation and the base plate, where it simulates the rising and the slip of the base plate and where friction at the interface concrete foundation–base plate is ensured by four-nodal quadratic elements [26]. The model has been elaborated in CASTEM3M computer code. The aim of this study is the analysis of the behavior of the most frequently used column–base plate connections. For this purpose, the curves of rising versus rotations and normal displacement versus tangential displacement are plotted.

2. **Unilateral Contact (the Signorini Problem)**. In numerous simulations, the law of unilateral contact used is illustrated by the Signorini problem. Consider a deformable body in contact with a rigid body (Fig. 1), the conditions of unilateral contact of the Signorini problem have to be satisfied in all points of the deformable bodies located in the contact Γ_C [27]:

$$h \le 0, \tag{1}$$

$$R_{\vec{n}} \le 0, \tag{2}$$

$$h \cdot R_{\vec{n}} = 0, \tag{3}$$

where h is the displacement of a point of contact in the normal direction to the contact, $\vec{n}$, while $R_{\vec{n}}$ are the normal effort components. Equation (1) represents the condition of impenetrability; Eq. (2) – the fact that the normal force of contact is compression, and Eq. (3) represents the condition of complementarity (if the point is in contact, then $h = 0$ and $R_{\vec{n}} \le 0$; if the point leaves the contact then $h \prec 0$ and $R_{\vec{n}} = 0$) [27].

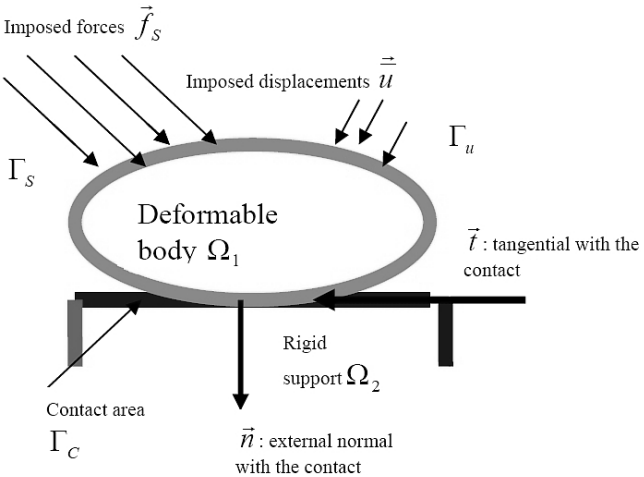

Fig. 1. Contact between a deformable body and a rigid body (the Signorini problem).

3. **Coulomb Law**. The force at the point of contact can be split into the normal force $R_{\vec{n}}$ and the tangential force $R_{\vec{t}}$ ($\vec{R} = R_{\vec{n}} \cdot \vec{n} + R_{\vec{t}} \cdot \vec{t}$). The model of Coulomb friction is written as follows [27]:

$$|R_{\vec{t}}| \le \mu |R_{\vec{n}}|, \tag{4}$$

$$|R_{\vec{t}}| \prec \mu |R_{\vec{n}}| \Rightarrow v_{\vec{t}} = 0 \qquad \text{(adherence)}, \tag{5}$$

$$R_{\vec{t}} = -\mu |R_{\vec{n}}| \frac{v_{\vec{t}}}{|v_{\vec{t}}|} \qquad \text{(slip)} \tag{6}$$

where $v_{\vec{t}}$ is tangential relative speed between the two bodies and μ is the Coulomb friction coefficient (see Fig. 2,) which includes all the local parameters, such as roughness of surface between the two bodies.

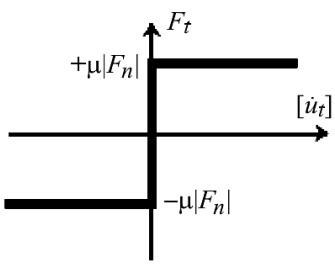

Fig. 2. Coulomb law.

4. **Equilibrium without Friction**. The deformable body is designated by Ω_1 and the rigid body- by Ω_2, while combination of the two bodies is $\Omega = \Omega_1 \cup \Omega_2$. The deformable body is subjected to action of the imposed displacements $\vec{u}_d$ in zone Γ_u, the imposed efforts $\vec{f}_S$ in zone Γ_σ, and bulk forces $\vec{f}_V$ acting in the field (Fig. 1):

$$\operatorname{div}\vec{\sigma} + \vec{f}_v = 0 \qquad \text{in } \Omega, \tag{7}$$

$$\vec{u} = \vec{u}_d \qquad \text{on } \Gamma_u, \tag{8}$$

$$[\sigma]\cdot\vec{n} = \vec{f}_S \qquad \text{on } \Gamma_\sigma, \tag{9}$$

$$[\sigma]\cdot\vec{n} = \vec{R} \qquad \text{on } \Gamma_C. \tag{10}$$

5. **Equilibrium with Friction**. Equilibrium of deformable body with frictional contact is written:

$$W_{solid} = \frac{1}{2}\int_V [\sigma]:\{\varepsilon\}dV - \int_V \vec{f}_V\cdot\vec{u}dV - \int_{\Gamma_C}\vec{f}_S\cdot\vec{u}dS - W_{cont}. \tag{11}$$

The work of contact forces in the deformable body is written as follows:

$$W_{cont} = \int\int_{\Gamma_C}(R_n\vec{n}\cdot\vec{u}_n + \vec{R}_t\cdot\vec{u}_t)dS \tag{12}$$

where $\vec{u}_t = (\vec{u}_2 - \vec{u}_1) - \vec{u}_n\cdot\vec{n}$.

The action of rigid body Ω_2 on body Ω_1 is written as

$$\vec{f}_{cont} = \int\int_{\Gamma_C}(R_n\cdot\vec{n} + \vec{R}_t)dS. \tag{13}$$

6. **Finite Element Modeling**.

Behavior law: $\sigma = C:\varepsilon$.

Interpolation of deformations: $\varepsilon = [B]\cdot u$.

Interpolation of displacements: $u = [N]\cdot u^k$.

In matrix form, Eq. (11) is written as

$$W_{solid} = \left(\frac{1}{2}u^T[K]\cdot u - u^T\{F\}\right) \tag{14}$$

with rigidity matrix

$$[K] = \int_V B^T[C]BdV$$

and external efforts' vector

$$\{F\} = \int_V [N^T]\vec{f}_V\, dV + \int_{\Gamma_C} [N^T]\vec{f}_S\, dS + \int_{\Gamma_C} [N^T]\vec{f}_{cont}\, dS\{F\}.$$

The system equilibrium with frictional contact aims to minimize the energy equation under the following constraint:

$$\begin{cases} \operatorname{div}\sigma \equiv \delta W_{solid} = 0, \\ h = ((\vec{u}_2 - \vec{u}_1)\cdot \vec{n} = [G]^T u_n = 0. \end{cases} \tag{15}$$

7. **Method of Resolution (Modified Lagrangian)**:

$$W_{solid}(u, \lambda) = \frac{1}{2} u^T [K] u + \lambda^T [G]^T u + \frac{\alpha}{2} u^T [G][G]^T u = 0, \tag{16}$$

$$\delta W_{solid}(u, \lambda) = 0 \Rightarrow \begin{cases} \dfrac{\partial W}{\partial u} = 0, \\ \dfrac{\partial W}{\partial \lambda} = 0, \end{cases} \Rightarrow \begin{cases} [K + \alpha G G^T] u^K + [G]\lambda^K = F, \\ \lambda^{K+1} = \lambda^K + \alpha [G]^T u^K. \end{cases} \tag{17}$$

8. **Behavior Laws**. For the adopted finite elements model of the column, the base plate and anchor bolts obey the laws depicted in Figs. 3 and 4.

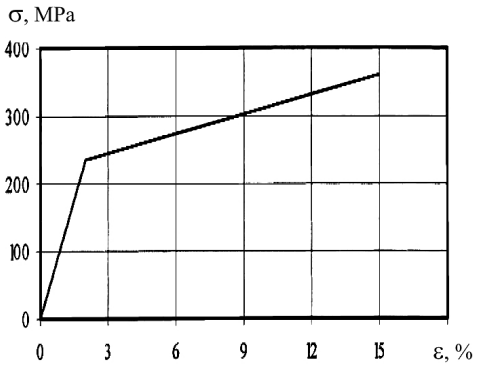

Fig. 3

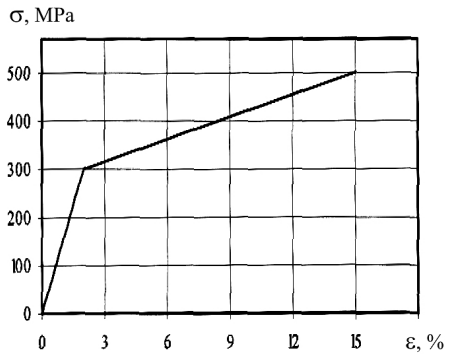

Fig. 4

Fig. 3. Adopted stress–strain relations for the steel column and base plate connection.
Fig. 4. Adopted stress–strain relations for the anchor bolts.

For the foundation concrete, the material is considered which operates in the elasto-plastic field with the Young modulus $E_C = 29$ GPa, Poisson's ratio $\gamma_C = 0.18$, the tensile strength $f_t = 3.0$ MPa, and the compressive strength $f_c = 38$ MPa.

9. **Numerical Analysis**. Three types of connections are studied, the first one consisting of a base plate ($t_p = 11$ mm) welded to the end of column and attached to the reinforced concrete foundation with two anchor bolts. These bolts are placed on the major axis of the I-shaped column cross section, one anchor bolt on each

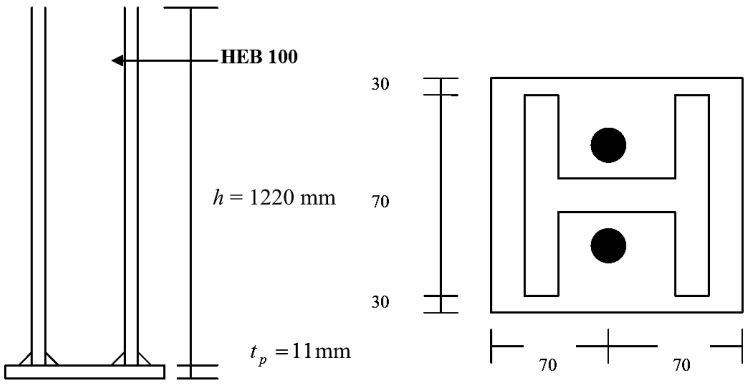

Fig. 5. Detail of two anchor bolts connection.

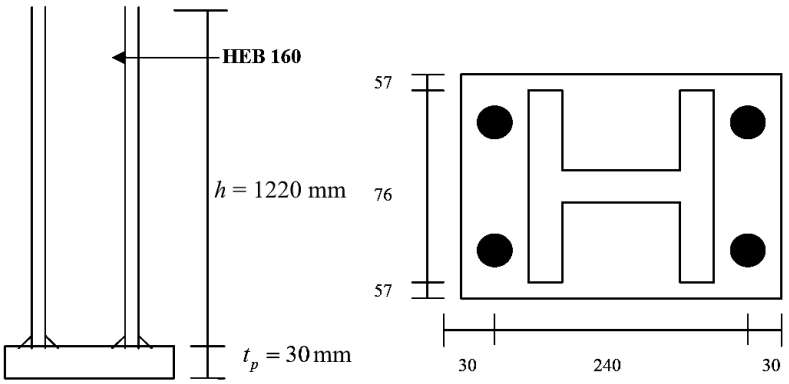

Fig. 6. Detail of four anchor bolts connection.

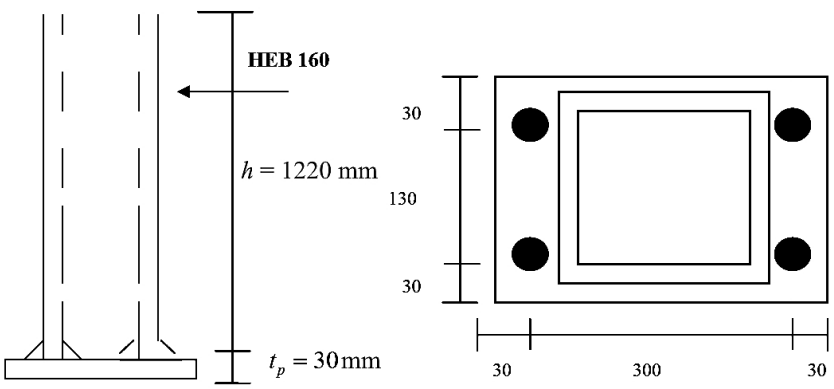

Fig. 7. Detail of four anchor bolts connection with a hollow cross section.

side of the web (Fig. 5). In the second configuration, the connection comprises a base plate ($t_p = 30$ mm) and four anchor bolts placed outside the flanges of the I-shaped section (Fig. 6). In the third configuration, the connection comprises a base plate ($t_p = 19$ mm), a column with a hollow cross section and four anchor bolts (Fig. 7). Two loading types are used. Initially, the connections were subjected to shear force and bending moment only, and then the connections were loaded by shear force, bending moment and axial compressive force (Fig. 8). In this case,

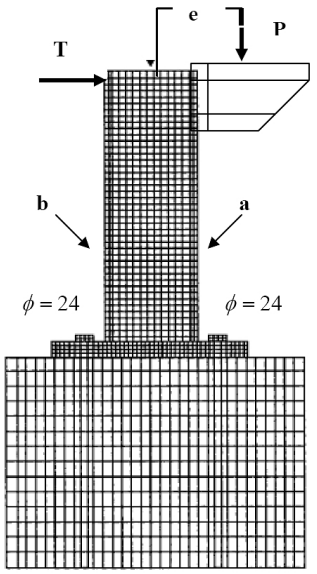

Fig. 8. Finite element mesh of the 3D model.

bending moment is induced by the offset compressive load. Different eccentricities and variable axial loadings ($P = 100$ to 600 kN) are chosen, in order to show the influence of these parameters on the degree of fixity of the column base connections. In this study, the following assumptions were made, in order to obtain essential response features:

1) An interaction between the holes in the base plate and the anchor bolts is ensured by considering a unilateral contact between these two bodies.

2) In order to simplify the mesh, the anchor bolts that are of circular sections are simulated in this study by bolts of square sections of equivalent surface.

3) The displacement of the anchor bolts is postulated so that the nodes coincide with the nodes of the holes of the base plate.

4) To take into account the contact friction between the base plate and the foundation, the nodes, as well as the degrees of freedom of the two bodies, are selected in a such way that they coincide.

5). The same precaution is also taken with regard to the nodes and the degrees of freedom of the anchor bolts and the concrete foundation.

6). Traction in the concrete develops only in the upper part of bolt (on the one third of L_P).

7). The loadings are introduced in the forms of increments (ensured well by CASTEM3M code).

10. **Results**. For the column–base plate connection with only two anchor bolts without compressive load rising of the base plate side of traction occurs. The anchor bolts undergo elongation and bending. The columns manifest no deformation; all rotation occurs at the level of connection.

For the same connection with two anchor bolts in the presence of compressive load ($P = 100$–400 kN), the rising of the base plate side of traction is still quite pronounced, but less critical (reduction from 6 to 16%). We observe that a contact zone is established under the right edge of the base plate. The remaining part of the

plate starts to separate from concrete foundation, overstressing the left bolt. The deformation of the base plate, as well as the plastic strains, decreases as axial load increases.

For the column–base plate connection with four anchor bolts without a compressive load: rupture of two anchor bolts in traction occurs. The base plate is raised considerably before the rupture of the anchor bolts. Rising maxima are 36, 32, and 29 mm, respectively, for the base plate thickness $t_p = 11$ mm (Figs. 9 and 10), 19 mm (Fig. 11), and 30 mm (Fig. 12). Comparing the results obtained with the model for base plate thickness $t_p = 30$ mm to those with base plate thickness $t_p = 11$ mm, the highest uplift is slightly smaller, as well as the separation length. These results are natural, since the stiffness of the base plate increases for thickness $t_p = 30$ mm, permitting smaller deformability and reducing its final plastic strain.

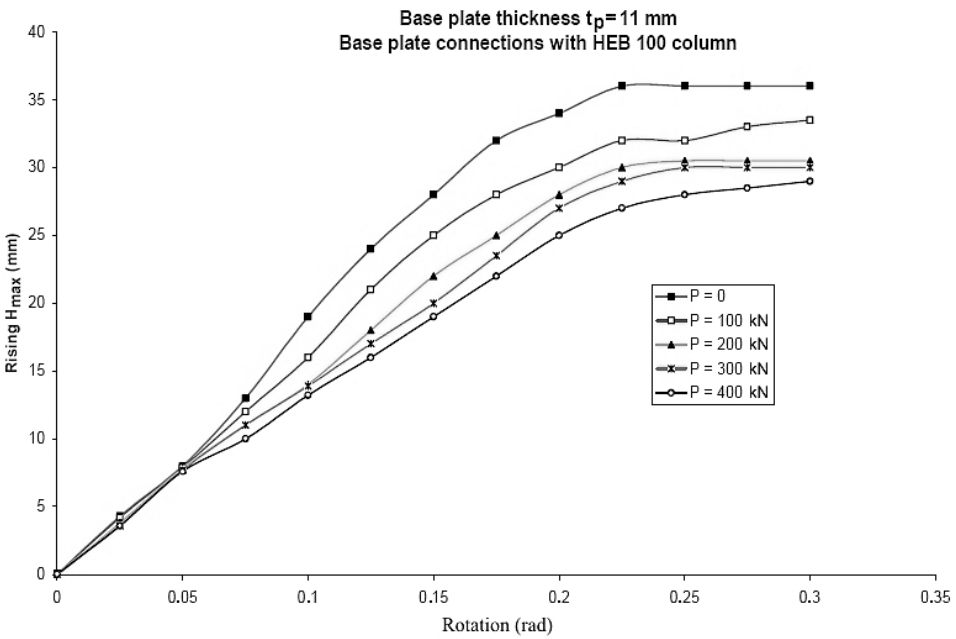

Fig. 9. Maximum rising-rotation diagrams for base plate thickness $t_p = 11$ mm under various axial loadings. Base plate connections with HEB 100 column.

On the compression side, there is friction of the base plate over 80 mm distance from the base plate edge. The columns remained practically rectilinear.

The results obtained for the same connections (HEB 160 with four anchor bolts) in the presence of compressive load (P = 100–600 kN) are as follows.

The rising of base plate is less visible than when there is no compressive load.

The contact area increases along with the axial loading from 0 to 600 kN.

We observe that the bending of the base plate is reduced in comparison with the connection without compressive load. This proves that the increase of the stiffness of the base plate significantly affects its response under applied axial loading and bending moment combination.

The rising of base plate side of traction becomes less critical when the compressive load increases. The reduction of the maximum rising is of the order of

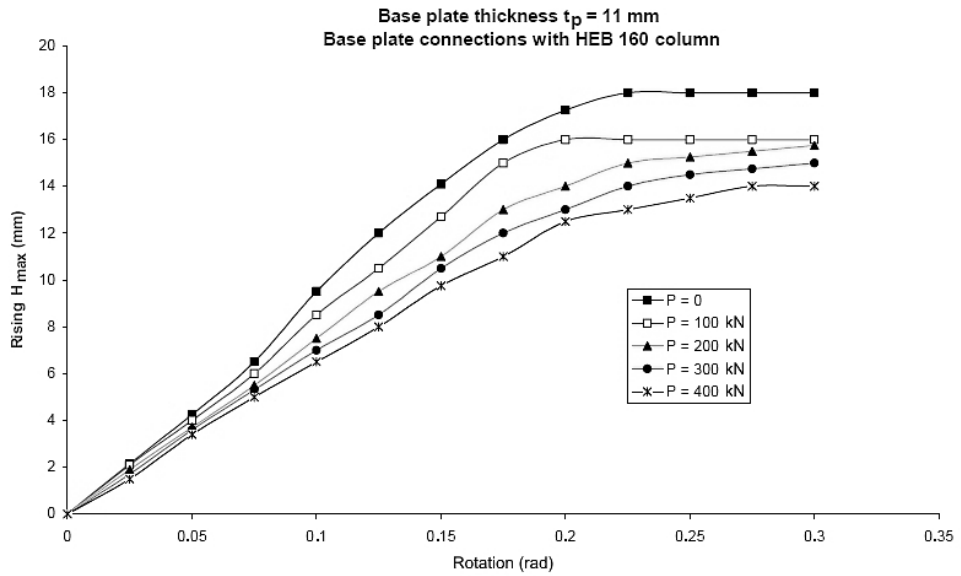

Fig. 10. Maximum rising-rotation diagrams for base plate thickness $t_p = 11$ mm under various axial loadings. Base plate connections with HEB 160 column.

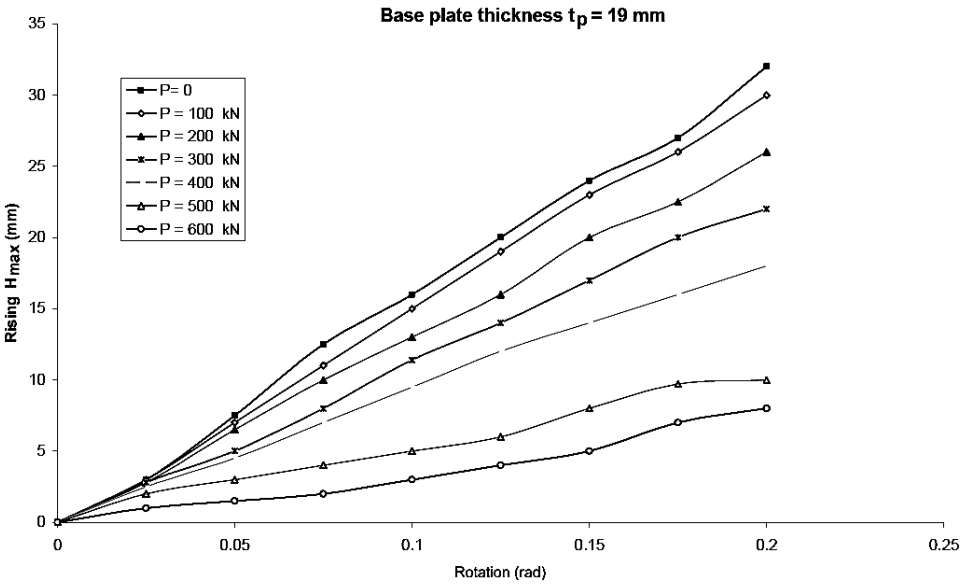

Fig. 11. Curves of the rising of the 19 mm thickness base plate under various axial loadings. Base plate connections with HEB 160 column.

magnitude (6 to 70%) while passing from compressive load of $P = 100$ kN to $P = 600$ kN.

Local warping of the wing in compression is observed.

Traction at the base of column is located at the same side as the wing in compression at the top of column. This is an indication that a moment is developed in the connection and the column works in double curve.

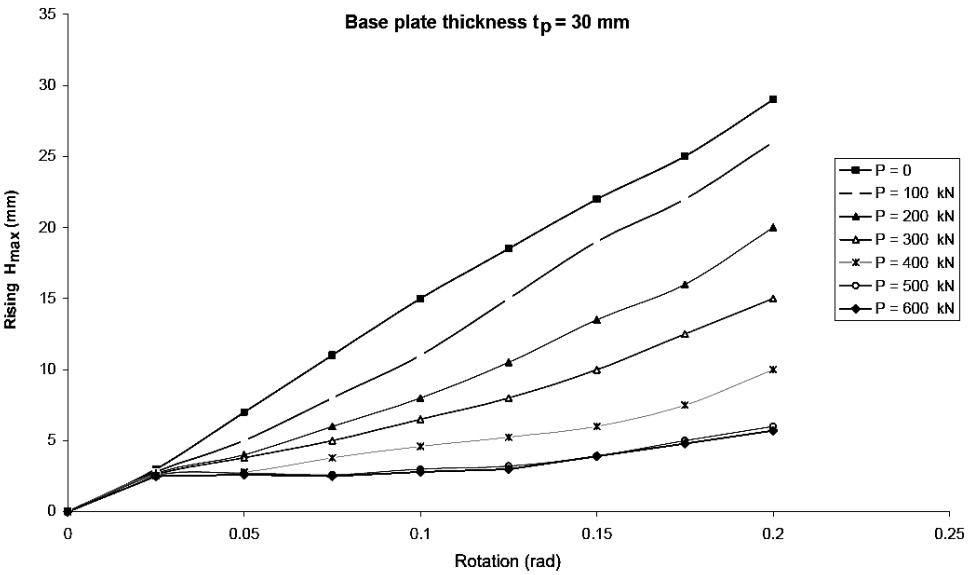

Fig. 12. Curves of the rising of the 30 mm thickness base plate under various axial loadings.

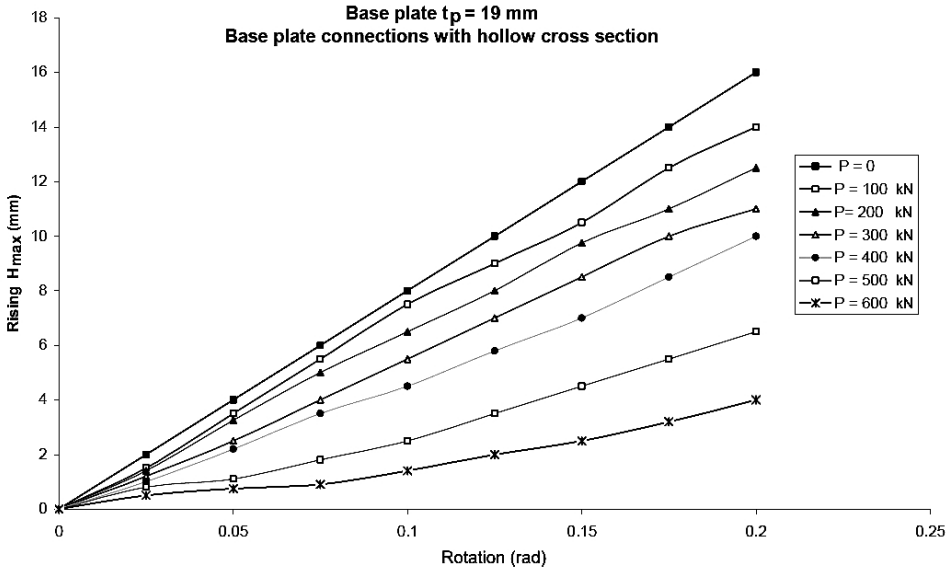

Fig. 13. Curves of the rising of the 19 mm thickness base plate under various axial loadings. Base plate connections with a hollow cross section.

For the connections with a hollow cross section, the rising of base plate is even less pronounced (Fig. 13).

Increasing the base plate thickness, the respective stiffness ensures limited deformation which manifests itself only slightly (Figs. 14–16).

Conclusions. To study the rising of the base plate, an approach treating problems of contact friction between the base plate and the foundation has been developed. The numerical solution is obtaiined by the modified Lagrangian method. For the account of the concrete foundation behavior, the developed model is based on the compressive elasto-plastic model.

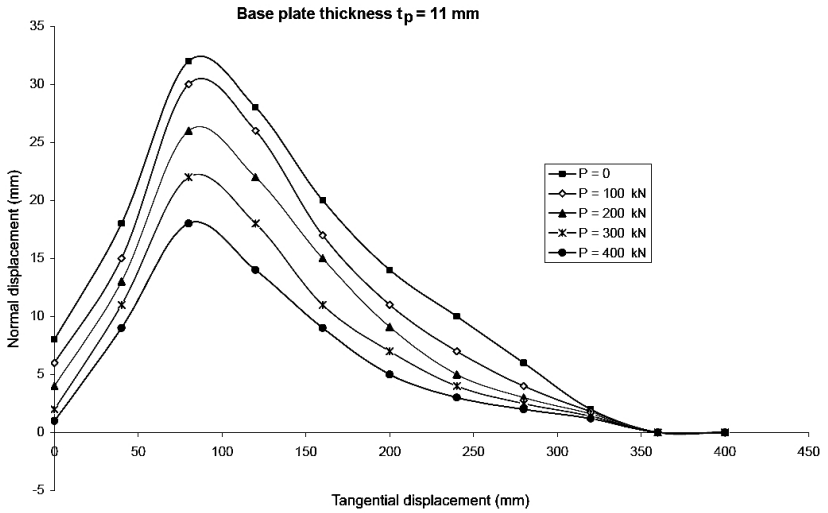

Fig. 14. Curves of the normal and tangential displacement of the 11 mm thickness base plate.

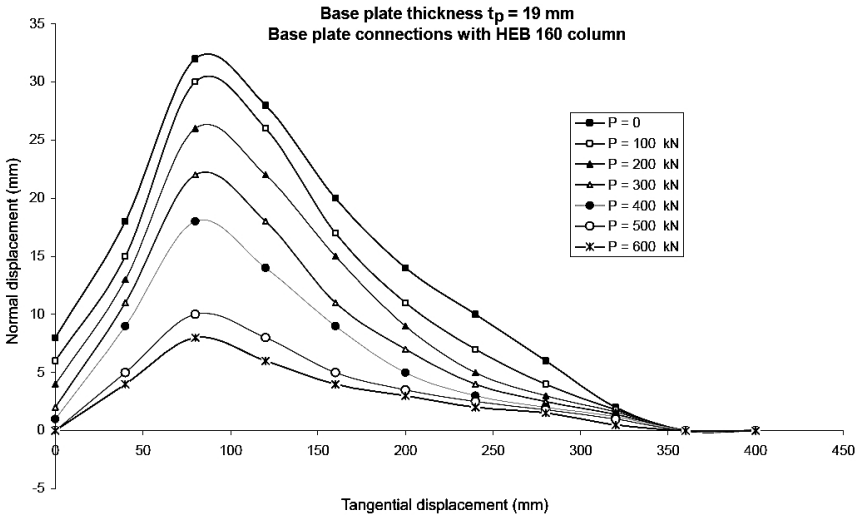

Fig. 15. Curves of the normal and tangential displacement of the 19 mm thickness base plate.

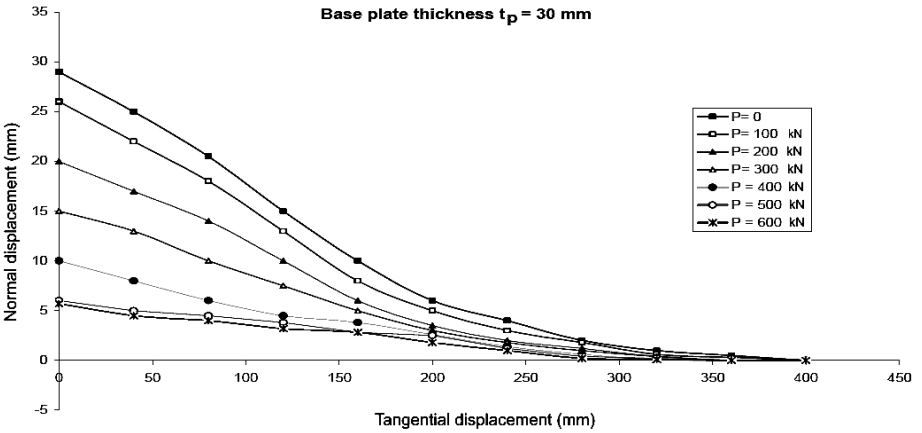

Fig. 16. Curves of the normal and tangential displacement of the 30 mm thickness base plate.

Р е з ю м е

Запропоновано скінченноелементну методику розрахунку деформування і відносного проковзування кріплень стальної колони до залізобетонної основи. Розглянуто два випадки кріплення: пластина приварюється до торця колони і кріпиться двома або чотирма анкерними болтами до залізобетонної основи. У скінченноелементній моделі з використанням модифікованого методу Лагранжа враховується розтріскування бетонної основи й ефекти тертя. Деформування бетонної основи описується за допомогою пружно-пластичної моделі стиску матеріалу. За результатами розрахунків побудовано діаграми переміщень елементів кріплення.

1. F. W. Stockwell, Jr., "Preliminary base plate selection," *Eng. J. AISC*, **12**, No. 3, 92–99 (1975).
2. B. S. Sandhu, "Steel column base plate design," *Ibid*, **10**, No. 4, 131–133 (1973).
3. W. R. Bird, "Rapid selection of column base plate," *Ibid*, **13**, No. 2, 43–47 (1976).
4. *Regles de Calcul des Constructions en Acier et Additive 80*, 12éme edition (1988).
5. *Eurocode 3. Design of Steel Structures. 1.1. General Rules for Building*, Env 1993-1-1 (1992).
6. A. Picard et J. Dion, *Etude Expérimentale des Assemblages Poteau–Fondation dans les Charpentes d'Acier*, Report GCT-81-04, Department of Civil Engineering, Laval University, Quebec (1981).
7. G. Samson et D. Beaulieu, *Etude de la Stabilité d'Un Poteau avec Attache Semi-Rigide à la Fondation*, Report GCT-83-01, Department of Civil Engineering, Laval University, Quebec (1982).
8. B. Pérusse et D. Beaulieu, *Etude Expérimentale de la Rigidité d'Un Assemblage Poteau–Fondation de Type Standard*, Report GCT-85-07, Department of Civil Engineering, Laval University, Quebec (1985).
9. J. T. Dewolfe, "Axially loaded column base plates," *J. Struct. Div. ASCE*, **104**, 781–794 (1978).
10. J. T. Dewolfe and E. F. Sansely, "Columnbase plates with axial loads and moments," *Ibid*, **106**, 2167–2184 (1983).
11. D. P. Thambiratnam and P. Paramasivan, "Base plates under axial loads and moments," *Ibid*, **112**, 1166–1181 (1986).
12. R. A. Cook and R. E. Klinger, "Ductile multiple-anchor steel-to-concrete connections," *Ibid*, **118**, 1645–1665 (1992).
13. R. S. Fling, "Design of steel bearing plates," *Eng. J. AISC*, **7**, 37–40 (1970).
14. T. M. Murray, "Design of lightly loaded steel column base plates," *Ibid*, **20**, 92–99, 143–152 (1983).

15. N. Krishnnamurthy and D. D. Graddy, “Correlation between 2- and 3-dimensional finite element analysis of steel bolted end-plate connections,” *Comput. Struct*., **6**, 381–389 (1976).

16. M. Hamizi et N. E. Hannachi, “Evaluation par la méthode des éléments finis du facteur de flexibilité et du degré de fixité des pieds de poteaux les plus couramment utilisés,” *Annales du Batiment et des Travaux Publics*, No. 2-3 (2007).

17. N. Krishnnamurthy, “A fresh look at bolted steel end-plate behavior and design,” *Eng. J. AISC*, **15**, 39–49 (1978).

18. B. Kato and W McGuire, “Analysis of T stub flange to column connection,” *J. Struct. Div. ASCE*, **99**, 865–888 (1973).

19. S. A. Paker and L. J. Morris, “A limit state design method for tension of bolted column connections,” *Struct. Eng*., **55**, 876–889 (1977).

20. A. R. Kukreti, T. M. Muray, and A. Abolmaali, “Endplate connection moment-rotation relationship,” *Struct. Steel Res*., **8**, 137–157 (1987).

21. W. F. Chen and K. V. Patel, “Static behaviour of beam-to-column moment,” *J. Struct. Div. ASCE*, **197**, 1815–1838 (1981).

22. W. F. Chen and E. M. Lui, “Steel beam-to-column moment connections. Pt. 1. Flange moment connections,” *S. M. Arch*., **11**, 257–316 (1986).

23. J. Bortmann and B. A. Szabo, “Nonlinear models for fastened structural connections,” *Comput. Struct*., **43**, 909–1023 (1992).

24. D. P. Thambiratnam and N. Krishnnamurthy, “Computer analysis of column base plates,” *Ibid*, **33**, 839–850 (1989).

25. C. C. Baniotopoulos, G. Karoumbas, and P. D. Panagiotopoulos, “A contribution to the analysis of steel connections by means of quadratic programming techniques,” in: Proc. of 1st Eur. Conf. on *Numerical Methods in Engineering*, Elsevier, Amsterdam (1992), pp. 519–525.

26. M. Hamizi et D. Beaulieu, *Etudes Expérimentale et Numérique des Pontages Métalliques*, Report GCT-87-05, Department of Civil Engineering, Laval University, Quebec (1987).

27. L. Champaney, *Contact Unilatéral entre Solides Élastiques. Notes de Cours ‘Eléments Finis’ du DESS Dynamique des Structures Modernes dans leur Environnement*.

Received 25. 05. 2010